Chemical Science

EDGE ARTICLE

View Article Online
View Journal | View Issue

Cite this: *Chem. Sci.*, 2015, **6**, 6496

Catalytic two-electron reduction of dioxygen catalysed by metal-free [14]triphyrin(2.1.1)†

Kentaro Mase,[a] Kei Ohkubo,[ab] Zhaoli Xue,[c] Hiroko Yamada*[c] and Shunichi Fukuzumi*[abd]

Received 8th July 2015
Accepted 2nd August 2015

DOI: 10.1039/c5sc02465j

www.rsc.org/chemicalscience

The catalytic two-electron reduction of dioxygen (O_2) by octamethylferrocene (Me_8Fc) occurs with a metal-free triphyrin (HTrip) in the presence of perchloric acid ($HClO_4$) in benzonitrile (PhCN) at 298 K to yield Me_8Fc^+ and H_2O_2. Detailed kinetic analysis has revealed that the catalytic two-electron reduction of O_2 by Me_8Fc with HTrip proceeds *via* proton-coupled electron transfer from Me_8Fc to HTrip to produce $H_3Trip^{\bullet+}$, followed by a second electron transfer from Me_8Fc to $H_3Trip^{\bullet+}$ to produce H_3Trip, which is oxidized by O_2 *via* formation of the H_3Trip/O_2 complex to yield H_2O_2. The rate-determining step in the catalytic cycle is hydrogen atom transfer from H_3Trip to O_2 in the H_3Trip/O_2 complex to produce the radical pair ($H_3Trip^{\bullet+}$ $HO_2^{\bullet}$) as an intermediate, which was detected as a triplet EPR signal with fine-structure by the EPR measurements at low temperature. The distance between the two unpaired electrons in the radical pair was determined to be 4.9 Å from the zero-field splitting constant (*D*).

Introduction

Utilization of natural energy to produce chemical energy consisting of earth-abundant elements is an essential technology for building a society based on the sustainable use of materials. Hydrogen peroxide (H_2O_2) produced by two-electron reduction of O_2 is a versatile and environmentally benign oxidant, which is widely used on a large industrial scale.[1,2] Furthermore, H_2O_2 has been proposed as a sustainable energy carrier that can be used in fuel cells, where direct and efficient conversion of chemical to electrical energy is required.[3–5] However, the anthraquinone process, currently used to produce H_2O_2 in industry, requires potentially explosive hydrogen and a noble metal catalyst.[6] Extensive efforts have so far been devoted to provide an alternative way to produce H_2O_2 photochemically or thermally without the use of noble metal catalysts.[7–13] In many cases, redox-active transition metal-based complexes such as cobalt,[14–23] iron,[24–27] and copper complexes,[28–31] have been employed as O_2 reduction catalysts, because triplet O_2 is inactive towards organic compounds due to spin restriction in the absence of an appropriate catalyst.[32]

Recently, nitrogen-doped carbon materials have attracted increasing attention as an efficient metal-free catalyst for the catalytic reduction of O_2.[33–35] However, the catalytic mechanism has yet to be well understood, because few spectroscopic studies to detect reaction intermediates in a catalytic cycle have been performed on heterogeneous systems. In homogeneous systems, reduced flavin analogues involved in flavoenzymes have so far been known to play a pivotal role in the catalytic reduction of O_2, which is a key step of biological oxidation.[36,37] In particular, the deprotonated states of reduced flavin analogues, which are thermodynamically more able to reduce O_2 *via* an electron-transfer process, are considered to be a reactive intermediate in the reduction of O_2.[38]

On the other hand, Girault and coworkers recently reported that the free base porphyrin has the ability to catalyse the two-electron reduction of O_2 using one-electron reductants such as ferrocene at liquid–liquid interfaces.[39] In such systems, although the catalytic mechanism of metal-free organocatalysts has yet to be clarified, the oxidation state of the organocatalyst is thought to remain the same during the catalytic reduction of O_2. Thus, no electron-transfer reduction of organic catalysts has been reported in relation to the catalytic reduction of O_2.

In this context, Nocera and coworkers recently reported the stabilization of the peroxide dianion within the cavity of a hexacarboxamide cryptand,[40] where strong hydrogen bond donors are arranged to completely surround the peroxide dianion with a partial positive charge. This result provides support for the proposal that metal-free organocatalysts, which have multiple hydrogen bonding moieties, can efficiently catalyse O_2 reduction.

[a]*Department of Material and Life Science, Graduate School of Engineering, ALCA and SENTAN, Japan Science and Technology Agency (JST), Osaka University, Suita, Osaka 565-0871, Japan. E-mail: fukuzumi@chem.eng.osaka-u.ac.jp*

[b]*Department of Chemistry and Nano Science, Ewha Womans University, Seoul 120-750, Korea*

[c]*Graduate School of Materials Science, Nara Institute of Science and Technology, CREST, Japan Science and Technology Agency (JST), Ikoma, Nara 630-0192, Japan. E-mail: hyamada@ms.naist.jp*

[d]*Faculty of Science and Engineering, ALCA, SENTAN, Japan Science and Technology Agency (JST), Meijo University, Nagoya, Aichi 468-0073, Japan*

† Electronic supplementary information (ESI) available: Spectroscopic, kinetic and DFT data. See DOI: 10.1039/c5sc02465j

We report herein the catalytic two-electron reduction of O_2 by an one-electron reductant, octamethylferrocene (Me_8Fc), with metal-free [14]triphyrin(2.1.1) (denoted as HTrip in Chart 1)[41] in the presence of $HClO_4$ in benzonitrile (PhCN) at 298 K. The catalytic mechanism for the O_2 reduction by Me_8Fc is clarified on the basis of a detailed kinetic study. Proton-coupled electron-transfer reduction of HTrip by Me_8Fc results in the formation of the reduced state of HTrip, and this resulting reduced HTrip is oxidized by O_2 to reproduce HTrip, indicating that HTrip acts as a metal-free catalyst for the reduction of O_2 by Me_8Fc in the presence of $HClO_4$ in PhCN. This discovery of a reactive intermediate in the catalytic O_2 reduction with a molecular organic catalyst provides valuable insight into the development of an efficient metal-free catalyst for the reduction of O_2.

Results and discussion

Protonation of HTrip with $HClO_4$

HTrip was protonated by addition of perchloric acid ($HClO_4$) to an air-saturated benzonitrile (PhCN) solution of HTrip. The characteristic absorption bands for HTrip at 524 and 581 nm decreased in intensity, with an increase in the absorption band at 565 nm, exhibiting clean isosbestic points, as shown in Fig. 1a. As can be seen in Fig. 1b, the absorbance change at 565 nm is saturated in the presence of 1 equiv. of $HClO_4$. Thus, HTrip is protonated to afford H_2Trip^+, as given by eqn (1).

$$HTrip + H^+ \rightarrow H_2Trip^+ \quad (1)$$

The pK_a value of H_2Trip^+ in PhCN was estimated to be 15.6 from the titration of HTrip with trifluoroacetic acid (TFA), as shown in Fig. S1 in the ESI.† The pK_a value of H_2Trip^+ is slightly larger than that of free base porphyrin analogues.[42] There is no further protonation due to strong repulsion between NH protons in the small macrocyclic ligand, as reported previously.[41]

Electrochemical measurements of HTrip in the presence of $HClO_4$

Electrochemical measurements of HTrip were performed in deaerated PhCN containing 0.10 M $TBAPF_6$, as shown in Fig. 2. A cyclic voltammogram of HTrip exhibits reversible reduction waves at $E_{1/2} = -1.13$ and -1.37 V (*vs.* SCE), which correspond to the first and second one-electron reduction of HTrip. The first

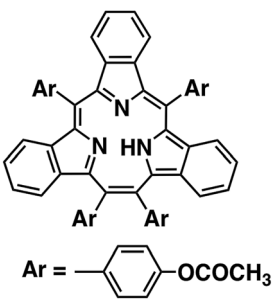

Chart 1 Structure of HTrip.

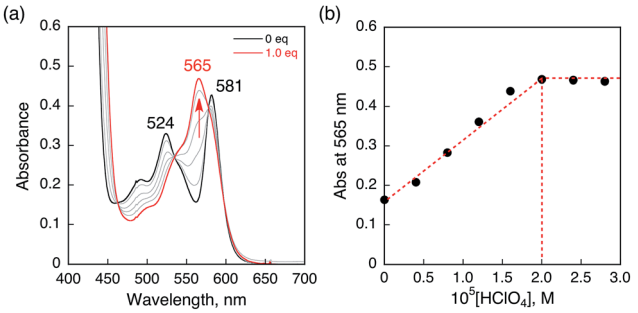

Fig. 1 (a) Absorption spectral changes of HTrip (2.0×10^{-5} M) upon the addition of $HClO_4$ in air-saturated PhCN at 298 K. (b) Absorbance change profile at 565 nm.

one-electron oxidation occurs at $E_{1/2} = 1.04$ V, which is followed by an irreversible oxidation (Fig. 2a). The formation of $HTrip^{\bullet-}$ was detected by UV-vis absorption spectra in the electrochemical reduction of HTrip at a controlled potential of -1.25 V *vs.* SCE in the thin-layer cell, as shown in Fig. S2 in the ESI.† By addition of $HClO_4$, the first reduction potential of HTrip was positively shifted from $E_{1/2} = -1.13$ V to -0.31 V (*vs.* SCE) because of the protonation of HTrip, but the reduction became irreversible (Fig. 2b). In such a case, proton-coupled electron transfer from an electron donor with the one-electron oxidation potential, which is less negative than -0.31 V, to HTrip may be thermodynamically feasible (*vide infra*).

Electron-transfer reduction of HTrip in the presence of $HClO_4$

No electron transfer from Me_8Fc to HTrip occurred in the absence of $HClO_4$ in PhCN at 298 K, as indicated by the more negative $E_{1/2}$ value of HTrip (-1.13 V *vs.* SCE) as compared with that of Me_8Fc (-0.04 V *vs.* SCE).[8] However, the addition of more than two equiv. of $HClO_4$ to a deaerated PhCN solution of Me_8Fc and HTrip resulted in the appearance of an absorption band at 738 nm due to H_3Trip with clean isosbestic points, as shown in Fig. 3. It should be noted that no electron transfer from Me_8Fc to H_2Trip^+ occurred in the presence of one equiv. of $HClO_4$, as shown in Fig. 3b. These results indicate that uphill electron transfer from Me_8Fc to H_2Trip^+ is coupled with protonation of $H_2Trip^{\bullet}$ to produce $H_3Trip^{\bullet+}$, followed by fast electron transfer from Me_8Fc to $H_3Trip^{\bullet+}$ to yield H_3Trip. Thus, the second protonation in fact occurs by coupling with reduction of H_2Trip^+ (*i.e.* $H_3Trip^{\bullet+}$ is accessible but not H_3Trip^{2+}). The stoichiometry of the overall reaction is given in Scheme 1.

The rate of proton-coupled electron-transfer reduction of H_2Trip^+ (k_{et}) to form $H_3Trip^{\bullet+}$ was determined from the dependence of the observed rate constant (k_{obs}) on concentrations of Me_8Fc and $HClO_4$, as shown in Fig. 4. The k_{obs} value was determined from the increase in absorbance at 738 nm due to H_3Trip, which obeyed first-order kinetics (Fig. S3 in the ESI†). The k_{obs} value increased linearly with increasing concentrations of Me_8Fc and $HClO_4$, as shown in Fig. 5. Thus, the rate of formation of H_3Trip is given by eqn (2).

$$d[H_3Trip]/dt = k_{et}[H_2Trip^+][HClO_4][Me_8Fc] \quad (2)$$

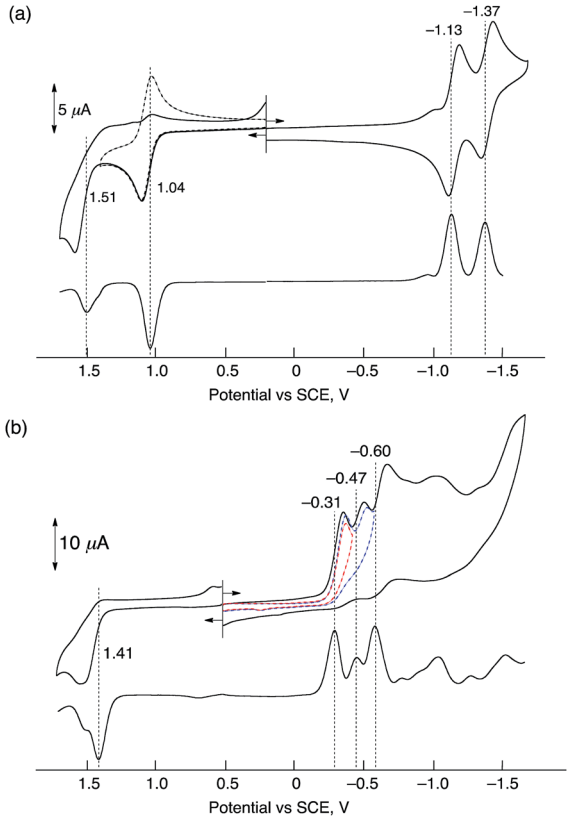

Fig. 2 Cyclic voltammograms (upper) and differential pulse voltammograms (lower) of deaerated PhCN solutions of HTrip (1.0×10^{-3} M) recorded in the presence of $TBAPF_6$ (0.10 M) (a) without $HClO_4$ and (b) with $HClO_4$ (1.0×10^{-2} M); sweep rate: 100 mV s^{-1} for CV and 4 mV s^{-1} for DPV.

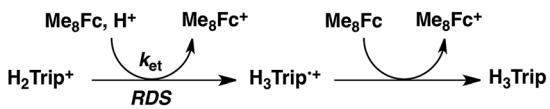

Scheme 1

The k_{et} value is determined from the slope of the linear plot of k_{obs} *vs.* [Me_8Fc] and [$HClO_4$] to be $(9.8 \pm 0.2) \times 10^4$ M^{-2} s^{-1}. The k_{et} value of the proton-coupled electron-transfer reduction of H_2Trip^+ by $Me_{10}Fc$ was also determined from the slope of the linear plot of k_{obs} *vs.* [$Me_{10}Fc$] and [$HClO_4$] to be $(3.1 \pm 0.3) \times 10^5$ M^{-2} s^{-1} (Fig. S4–S6 in the ESI†). The k_{et} value for $Me_{10}Fc$ is larger than that for Me_8Fc because $Me_{10}Fc$ ($E_{ox} = -0.08$ V *vs.* SCE) is a stronger electron donor than Me_8Fc (−0.04 V *vs.* SCE).[28]

The formation of H_3Trip was also confirmed by the electrochemical reduction of H_2Trip^+ monitored by the UV-vis spectral change at an applied potential of −0.30 V *vs.* SCE in the thin-layer cell, as shown in Fig. S7 (in the ESI†). The product obtained after the electrochemical reduction of H_2Trip^+ at −0.30 V displayed the characteristic absorption band at 738 nm. The same absorption band was seen in the chemical reduction of H_2Trip^+ by Me_8Fc in the presence of $HClO_4$ (Fig. 2).

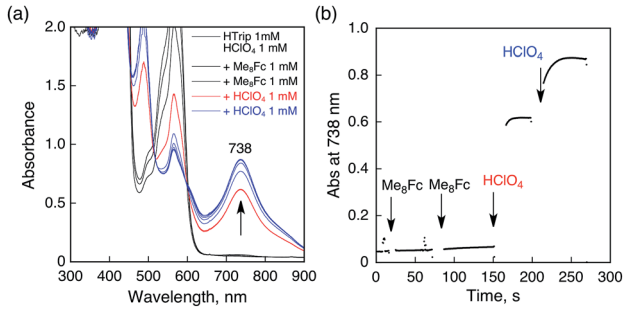

Fig. 3 (a) Absorption spectral changes upon addition of Me_8Fc (1.0×10^{-3} and 2.0×10^{-3} M) to a deaerated PhCN solution of H_2Trip^+ (1.0×10^{-3} M) in the presence of $HClO_4$ (1.0×10^{-3} M) at 298 K in a quartz cuvette (light path length = 1 mm) (black); absorption spectral change upon addition of $HClO_4$ (1.0×10^{-3} M) to the solution indicated by the black line (red); absorption spectral change upon addition of $HClO_4$ (1.0×10^{-3} M) to the solution indicated by the red line (blue). (b) Absorption change at 738 nm upon addition of various concentrations of Me_8Fc and $HClO_4$.

When O_2 was introduced to a deaerated PhCN solution of H_3Trip produced by the proton-coupled electron transfer from Me_8Fc to HTrip in the presence of $HClO_4$, the absorption band at 738 nm due to H_3Trip was immediately changed to a new absorption band at 720 nm, which can be attributed to the formation of the O_2 complex, as shown in Scheme 2 (*vide infra*). Subsequently, this spectrum decreased gradually, accompanied by the regeneration of HTrip as shown in Fig. 6. This indicates that H_3Trip was readily oxidized by O_2 to produce HTrip and H_2O_2 (Scheme 2).

Catalytic two-electron reduction of O_2 by Me_8Fc with HTrip in the presence of $HClO_4$

The proton-coupled electron-transfer reduction of HTrip by Me_8Fc (Scheme 1) and the oxidation of the resulting reduced HTrip (H_3Trip) by O_2 (Scheme 2) indicate that HTrip acts as a metal-free catalyst for the reduction of O_2 by Me_8Fc in the presence of $HClO_4$ in PhCN. Indeed, the addition of Me_8Fc to air-saturated PhCN at 298 K containing a catalytic amount of

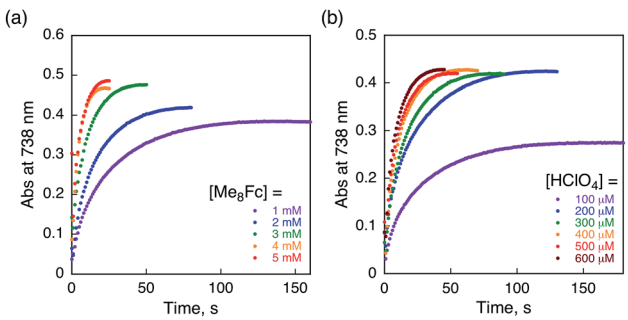

Fig. 4 Time profiles of absorbance at 738 nm due to H_3Trip in the reduction of H_2Trip^+ (2.5×10^{-5} M) (a) by various concentrations of Me_8Fc in the presence of $HClO_4$ (3.0×10^{-4} M) and (b) by Me_8Fc (2.0×10^{-3} M) in the presence of various concentrations of $HClO_4$ in deaerated PhCN at 298 K.

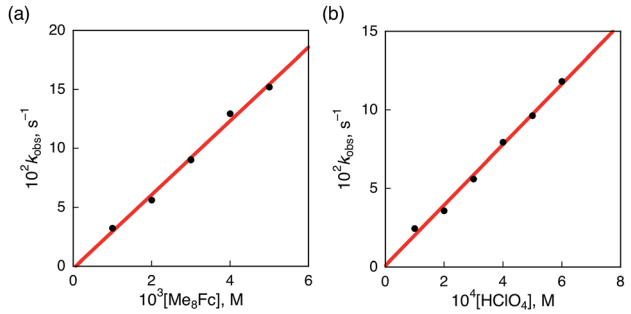

Fig. 5 (a) Plot of k_{obs} *vs.* [Me_8Fc] for the reduction of H_2Trip^+ (2.5×10^{-5} M) by various concentrations of Me_8Fc in the presence of $HClO_4$ (3.0×10^{-4} M) in PhCN at 298 K. (b) Plot of k_{obs} *vs.* [$HClO_4$] for the reduction of H_2Trip^+ (2.5×10^{-5} M) by Me_8Fc (2.0×10^{-3} M) in the presence of various concentrations of $HClO_4$ in deaerated PhCN at 298 K.

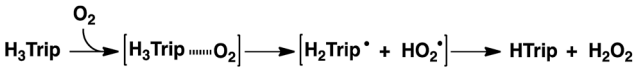

Scheme 2

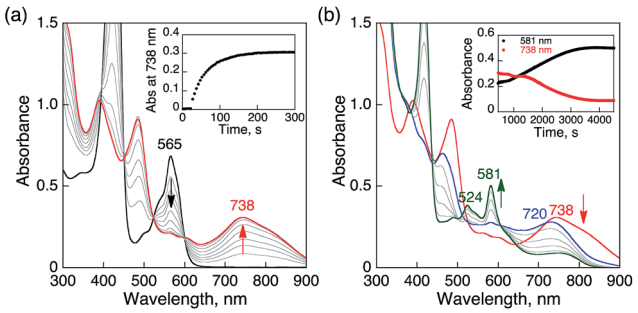

Fig. 6 (a) Absorption spectral changes produced by electron transfer from Me_8Fc (1.0×10^{-4} M) to HTrip (2.5×10^{-5} M) in the presence of $HClO_4$ (1.0×10^{-4} M) in deaerated PhCN at 298 K. (b) Absorption spectral changes upon introducing O_2 to a deaerated PhCN solution of (a). The red and green lines show the spectrum of H_3Trip before and after introducing O_2 by O_2 gas bubbling, respectively. The blue line shows the spectrum due to precursor complex. Insets show absorption time profiles.

HTrip and a large excess of $HClO_4$ resulted in the efficient oxidation of Me_8Fc by O_2 to yield Me_8Fc^+, as shown in Fig. 7a.

The formation of Me_8Fc^+ was monitored by a rise in absorbance at 750 nm due to Me_8Fc^+ (Fig. 7b). When an excess amount of Me_8Fc relative to O_2 (*i.e.*, [O_2] limiting conditions) was employed, the concentration of produced Me_8Fc^+ (1.9×10^{-3} M) was twice that of O_2 (9.4×10^{-4} M). In addition, the stoichiometric production of H_2O_2 was confirmed by iodometric titration, as shown in Fig. S8 (in the ESI†). In contrast, when an excess amount of O_2 relative to Me_8Fc (*i.e.*, [Me_8Fc] limiting conditions) was employed, the concentration of produced H_2O_2 (1.0×10^{-3} M) was half that of Me_8Fc (2.0×10^{-3} M), where the amount of H_2O_2 was determined by the reaction with $[(TMC)Fe^{II}](OTf)_2$ (TMC = 1,4,8,11-tetramethyl-

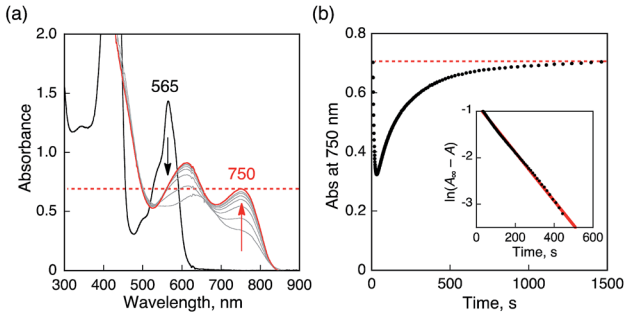

Fig. 7 (a) Absorption spectral changes in the two-electron reduction of O_2 (9.4×10^{-4} M) by Me_8Fc (1.0×10^{-2} M) with HTrip (5.0×10^{-5} M) in the presence of $HClO_4$ (1.0×10^{-2} M) in PhCN at 298 K. The black and red lines show the spectra before and after addition of Me_8Fc, respectively. The dotted line is the absorbance at 750 nm due to 1.9×10^{-3} M of Me_8Fc^+. (b) Time profile of absorbance at 750 nm due to Me_8Fc^+. Inset shows first-order plot.

1,4,8,11-tetraazacyclotetradecane) to produce the corresponding Fe(IV)-oxo complex $([TMC]Fe^{IV}(O))^{2+}$, as shown in Fig. S9 (in the ESI†).[43] Thus, the stoichiometry of the catalytic reduction of O_2 by Me_8Fc has been firmly established, as given in eqn (3).

$$O_2 + 2H^+ + 2Me_8Fc \xrightarrow[HTrip]{} H_2O_2 + 2Me_8Fc^+ \quad (3)$$

The rate of formation of Me_8Fc^+ in the catalytic reduction of O_2 with excess Me_8Fc and $HClO_4$ in Fig. 7b obeys first-order kinetics. It should be noted that the oxidation of Me_8Fc by O_2 hardly occurred in the absence of HTrip under the present experimental conditions, as shown in Fig. S10 (in the ESI†). When Me_8Fc was replaced by weaker one-electron reductants such as ferrocene (Fc : E_{ox} = 0.37 V *vs.* SCE) and dimethylferrocene (Me_2Fc : E_{ox} = 0.26 V *vs.* SCE), no changes in the absorption band of H_2Trip^+ at 565 nm were observed, as shown in Fig. S11 (in the ESI†). When Me_8Fc was replaced by a stronger one-electron reductant, *i.e.*, decamethylferrocene ($Me_{10}Fc$: E_{ox} = −0.10 V *vs.* SCE), greatly enhanced oxidation of $Me_{10}Fc$ occurred with the decrease in absorbance at 565 nm due to H_2Trip^+ (Fig. S12a in the ESI†). In the case of $Me_{10}Fc$, however, the oxidation of $Me_{10}Fc$ by O_2 occurred without HTrip in the presence of $HClO_4$ in PhCN (Fig. S12c in the ESI†). These results indicate that the reduction of H_2Trip^+ to produce H_3Trip is essential in the catalytic reduction of O_2 to produce H_2O_2.

When a metal complex of HTrip, η^5-cyclopentadienyliron(II) [14]triphyrin(2.1.1) ($CpFe^{II}Trip$),[41c] was employed as an O_2 reduction catalyst instead of HTrip for comparison, however, the addition of $HClO_4$ to an air-saturated PhCN solution of $CpFe^{II}Trip$ resulted in a spectral change, as shown in Fig. S13 (in the ESI†). The characteristic absorption bands of $CpFe^{II}Trip$ at 545 nm and 608 nm disappeared upon the addition of $HClO_4$ with the appearance of new absorption bands at 565 nm, which can be attributed to those of H_2Trip^+. This indicates that $CpFe^{II}Trip$ was easily demetallated and protonated to afford H_2Trip^+ in the presence of $HClO_4$, as shown in Fig. S13 (in the ESI†).

Kinetics and mechanism of the catalytic two-electron reduction of O_2 by Me_8Fc with HTrip

The dependence of the first-order rate constant for the formation of Me_8Fc^+ on the concentrations of HTrip, $HClO_4$, Me_8Fc, and O_2 was examined, as shown in Fig. S14 (in the ESI†), where the first-order rate constants were determined from the initial slopes of the first-order plots in order to avoid further complication due to the deactivation of the catalyst during the reactions, as shown in Fig. S15 (in the ESI†). The observed first-order rate constant (k_{obs}) was proportional to the concentration of HTrip, whereas the k_{obs} value remained constant irrespective of the concentration of $HClO_4$ or Me_8Fc (Fig. 8). Although no degradation of HTrip occurred under the present acidic conditions (Fig. S16 in the ESI†), the turnover number (TON) based on HTrip was determined to be more than 40 when the lower concentration of HTrip (1.3×10^{-5} M) was employed, as shown in Fig. S14a (in the ESI†). Because the catalytic rate depends only on the concentrations of HTrip and O_2, the rate-determining step in the catalytic cycle must be the reaction of H_3Trip with O_2 in Scheme 3. The dependence of the initial rate of formation of Me_8Fc^+ on the concentration of O_2 shows saturation behaviour at large concentrations of O_2 (Fig. 8d). Such saturation behaviour is consistent with the formation of the O_2 complex (H_3Trip/O_2) in the oxidation of H_3Trip with O_2 (Fig. 6b and Scheme 3). The overall catalytic cycle is shown in Scheme 3, where proton-coupled electron transfer from Me_8Fc to HTrip is followed by a second electron transfer from Me_8Fc to $H_3Trip^{\bullet+}$ to produce H_3Trip, which is slowly oxidized by O_2 *via* the H_3Trip/O_2 complex as the rate-determining step. Because the direct reaction between H_3Trip and O_2 in the H_3Trip/O_2 complex is spin-forbidden, the reaction may proceed *via* hydrogen atom transfer from H_3Trip to O_2 in the H_3Trip/O_2 complex to produce the ($H_2Trip^{\bullet}/HO_2^{\bullet}$) intermediate, followed by a rapid second hydrogen transfer from $H_2Trip^{\bullet}$ to $HO_2^{\bullet}$ to yield H_2O_2, accompanied by regeneration of HTrip (Scheme 3). According to Scheme 3, the rate of formation of Me_8Fc^+ is given by eqn (4),

$$d[Me_8Fc^+]/dt = k_{cat}[H_3Trip/O_2], \quad (4)$$

where k_{cat} is the rate constant of the hydrogen atom transfer from H_3Trip to O_2 in the H_3Trip/O_2 complex. Because the concentration of the H_3Trip/O_2 complex is given by eqn (5)

$$[H_3Trip/O_2] = K[HTrip][O_2]/(1 + K[O_2]), \quad (5)$$

using the formation constant (K), the initial concentration of HTrip, which is converted to H_3Trip in the catalytic reaction, and the concentration of O_2, eqn (4) is rewritten as eqn (6).

$$d[Me_8Fc^+]/dt = k_{cat}K[HTrip][O_2]/(1 + K[O_2]) \quad (6)$$

This kinetic equation agrees with the experimental observations in Fig. 8. The k_{cat} and K values were determined from the dependence of the catalytic rate on the concentration of O_2 (Fig. 8d) to be 0.5 s^{-1} and 8.4×10^2 M^{-1}, respectively.

Although the radical pair ($H_2Trip^{\bullet}/HO_2^{\bullet}$) in Scheme 3 cannot be detected during the catalytic reaction, the formation of the radical pair ($H_2Trip^{\bullet}/HO_2^{\bullet}$) was successfully detected by EPR measurements using 1-benzyl-1,4-dihydronicotinamide dimer [$(BNA)_2$][44] as an electron donor to produce H_3Trip under photoirradiation at low temperature. The observed EPR spectrum in aerated PhCN in the presence of $HClO_4$ at low temperature is shown in Fig. 9. A triplet fine structure EPR signal was observed as well as the typical anisotropic signals for $HO_2^{\bullet}$ with the $g_{||}$ value of 2.0341, and isotropic signals for $H_2Trip^{\bullet}$ at 2.0030.[45,46] From the zero-field splitting value (D = 230 G), the distance (r) between two unpaired electrons was determined using the relation $D = 27\ 800/r^3$ [47] to be 4.9 Å. This distance is consistent with the estimated distance between O_2 and H_3Trip in the H_3Trip/O_2 complex by DFT calculations (Fig. 9b).

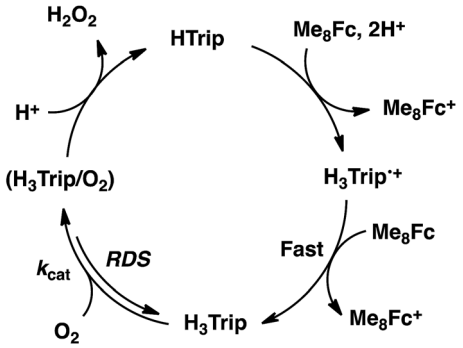

Scheme 3

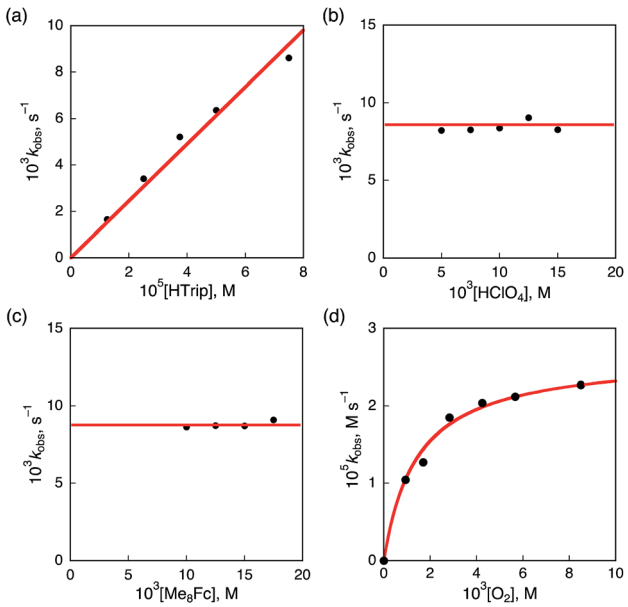

Fig. 8 Plots of (a) k_{obs} *vs.* [HTrip] for the two-electron reduction of O_2 (9.4×10^{-4} M) by Me_2Fc (1.0×10^{-2} M) with various concentrations of HTrip in the presence of $HClO_4$ (1.0×10^{-2} M) in PhCN; (b) k_{obs} *vs.* [$HClO_4$] for the two-electron reduction of O_2 (9.4×10^{-4} M) by Me_8Fc (1.0×10^{-2} M) with HTrip (5.0×10^{-5} M) in PhCN at 298 K; (c) k_{obs} *vs.* [Me_8Fc] for the two-electron reduction of O_2 (9.4×10^{-4} M) by various concentrations of Me_8Fc with HTrip (5.0×10^{-5} M) in the presence of $HClO_4$ (1.0×10^{-2} M) in PhCN at 298 K; and (d) k_{obs} *vs.* [O_2] for the two-electron reduction of O_2 by Me_8Fc (1.0×10^{-2} M) with HTrip (5.0×10^{-5} M) in the presence of $HClO_4$ (1.0×10^{-2} M) in PhCN at 298 K.

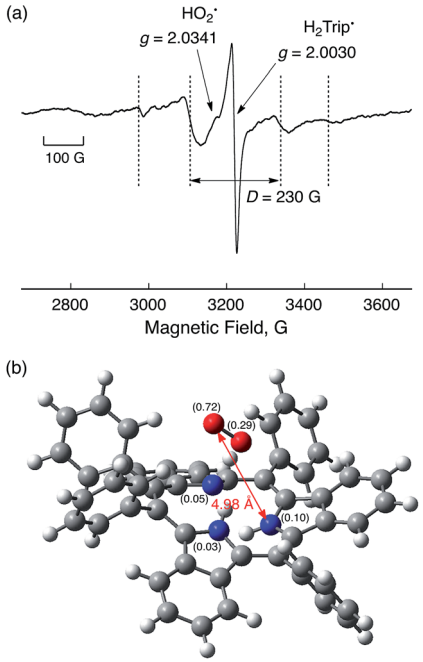

Fig. 9 EPR spectrum observed after the reduction of HTrip (1.0×10^{-3} M) by $(BNA)_2$ (2.0×10^{-3} M) in the presence of $HClO_4$ (1.0×10^{-3} M) in aerated PhCN under photoirradiation using a high-pressure Hg lamp (1000 W) measured at 80 K. Experimental conditions: Microwave frequency 9.0 GHz, microwave power 1.0 mW, modulation frequency 100 kHz, and modulation width 10 G. (b) Optimized structure of H_3Trip/O_2 calculated by DFT with calculated spin-density values given in parentheses at the UB3LYP/6-31G(d) level of theory.

Conclusion

Metal-free triphyrin acts as an efficient catalyst for the two-electron reduction of O_2 by Me_8Fc to produce H_2O_2 in the presence of $HClO_4$ in PhCN at 298 K. The rate-determining step (RDS) in the catalytic cycle has been found to be hydrogen atom transfer from H_3Tip to O_2 in the H_3Trip/O_2 complex to produce the radical pair ($H_3Trip^{\bullet+}/HO_2^{\bullet}$), which was detected as a triplet species by EPR at 80 K. The distance between the two unpaired electrons (4.9 Å) determined from the zero-field splitting constant (D) agrees with the distance in the H_3Trip/O_2 complex calculated by DFT. The present study provides valuable insight into the catalytic mechanism of the two-electron reduction of O_2 with an organic catalyst, and may lead to the development of more efficient metal-free organic catalysts for the selective two-electron reduction of O_2 to produce H_2O_2.

Experimental section

General procedure

Chemicals were purchased from commercial sources and used without further purification, unless otherwise noted. Perchloric acid ($HClO_4$, 70%), trifluoroacetic acid (TFA), ferrocene (Fc), and 1,1-dimethylferrocene (Me_2Fc) were purchased from Wako Pure Chemical Industries Ltd. Octamethylferrocene (Me_8Fc) and decamethylferrocene ($Me_{10}Fc$) were received from Sigma Aldrich. Fc, Me_2Fc, Me_8Fc, and $Me_{10}Fc$ were purified by sublimation or recrystallization from ethanol. Benzonitrile (PhCN) used for spectroscopic and electrochemical measurements was distilled over phosphorus pentoxide prior to use.[48] [14]Triphyrin(2.1.1) [HTrip] was synthesized according to the reported procedure.[41] Fe(II)(TMC)$(OTf)_2$ (TMC = 1,4,8,11-tetramethyl-1,4,8,11-tetraazacyclotetradecane; OTf = CF_3SO_3) was prepared according to a literature method.[43] Tetra-*n*-butylammonium hexafluorophosphate ($TBAPF_6$) was twice recrystallized from ethanol and dried *in vacuo* prior to use. ^1H NMR spectra (300 MHz) were recorded on a JEOL AL-300 spectrometer at room temperature and chemical shifts (ppm) were determined relative to tetramethylsilane (TMS). UV-vis absorption spectroscopy was carried out on a Hewlett Packard 8453 diode array spectrophotometer at room temperature using a quartz cell (light path length = 1 cm).

Spectroscopic measurements

The amount of hydrogen peroxide (H_2O_2) produced was determined by titration with iodide ion: a dilute CH_3CN solution (2.0 mL) of the product mixture (50 μL) was treated with an excess amount of NaI, and the amount of I_3^- formed was determined from the absorption spectrum ($\lambda_{max} = 361$ nm, $\varepsilon = 2.8 \times 10^4$ M^{-1} cm^{-1}).[49] The formation of H_2O_2 in the catalytic O_2 reduction with HTrip was again confirmed by the reaction between H_2O_2 and Fe(II)(TMC)$(OTf)_2$ to afford the corresponding Fe(IV)-oxo species. The amount of the Fe(IV)-oxo species produced was determined from the absorption spectrum ($\lambda_{max} = 820$ nm, $\varepsilon = 400$ M^{-1} cm^{-1}).[43]

The turnover numbers (TON = the number of moles of H_2O_2 formed per mole of HTrip in the catalytic two-electron reduction of O_2) were determined from the concentration of produced Me_8Fc^+ under catalytic conditions, where stoichiometric production of H_2O_2 was confirmed by iodometric titration.

Kinetic measurements

Rate constants of oxidation of ferrocene derivatives by O_2 in the presence of a catalytic amount of HTrip and an excess amount of $HClO_4$ in PhCN at 298 K were determined by monitoring the appearance of an absorption band due to the corresponding ferrocenium ions (Fc^+, $\lambda_{max} = 620$ nm, $\varepsilon_{max} = 330$ M^{-1} cm^{-1}; Me_2Fc^+, $\lambda_{max} = 650$ nm, $\varepsilon_{max} = 290$ M^{-1} cm^{-1}; Me_8Fc^+, $\lambda_{max} = 750$ nm, $\varepsilon_{max} = 410$ M^{-1} cm^{-1}; $Me_{10}Fc^+$, $\lambda_{max} = 780$ nm, $\varepsilon_{max} = 450$ M^{-1} cm^{-1}).[14] At the wavelengths monitored, spectral overlap was observed with H_3Trip ($\lambda = 738$ nm ($\varepsilon = 1.6 \times 10^3$ M^{-1} cm^{-1})), H_3Trip/O_2 ($\lambda = 720$ nm ($\varepsilon = 1.2 \times 10^3$ M^{-1} cm^{-1})). The concentration of O_2 in an air-saturated PhCN solution was determined to be 1.7×10^{-3} M as reported previously.[50] The concentrations of ferrocene derivatives employed for the catalytic reduction of O_2 were much larger than that of O_2, as O_2 is the rate-limiting reagent in the reaction solution. The PhCN solutions containing various concentrations of O_2 for the kinetic measurements were prepared by N_2/O_2 mixed gas bubbling using a KOFLOC GASBLENDER GB-3C. Typically, a PhCN stock solution of a ferrocene derivative was added using a

microsyringe to a PhCN solution containing HTrip and $HClO_4$ in a quartz cuvette (light path length = 1 cm).

Electrochemical measurements

Cyclic voltammetry (CV) measurements were performed on an ALS 630B electrochemical analyser and voltammograms were measured in deaerated PhCN containing 0.10 M $TBAPF_6$ as a supporting electrolyte at room temperature. A conventional three-electrode cell was used with a glassy carbon working electrode (surface area of 0.3 mm^2) and a platinum wire as the counter electrode. The glassy carbon working electrode (BAS) was routinely polished with BAS polishing alumina suspension and rinsed with acetone before use. The potentials were measured with respect to the $Ag/AgNO_3$ (1.0×10^{-2} M) reference electrode. All potentials (*vs.* $Ag/AgNO_3$) were converted to values *vs.* SCE by adding 0.29 V.[51] Redox potentials were determined using the relation $E_{1/2} = (E_{pa} + E_{pc})/2$.

Spectroelectrochemical measurements

UV-visible spectroelectrochemical experiments were performed with a home-built thin-layer cell (1 mm) that had a light transparent platinum net working electrode. Potentials were applied and monitored with an ALS 730D electrochemical analyser.

EPR measurements

EPR spectra were measured on a JEOL X-band EPR spectrometer (JES-ME-LX) using a quartz EPR tube containing a deaerated frozen sample solution at 80 K. The internal diameter of the EPR tube is 4.0 mm, which is small enough to fill the EPR cavity but large enough to obtain good signal-to-noise ratios during the EPR measurements at low temperatures (at 80 K). EPR spectrum of $HTrip^{\bullet -}$ produced by the electrochemical reduction of HTrip was measured using a home-built three-electrode quartz EPR tube. Potentials were applied and monitored with an ALS 730D electrochemical analyser. EPR spectra were measured under nonsaturating microwave power conditions. The amplitude of modulation was chosen to optimize the resolution and the signal-to-noise (S/N) ratio of the observed spectra. The g values were calibrated with a Mn^{2+} marker.

Theoretical calculations

Density functional theory (DFT) calculations were performed on a 32CPU workstation (PQS, Quantum Cube QS8-2400C-064). Geometry optimisations were carried out using the B3LYP/6-31G(d) level of theory[52] for $HTrip^{\bullet -}$, H_2Trip^{+}, H_3Trip^{2+}, $H_3Trip^{\bullet +}$, and $[H_3Trip/O_2]$. All calculations were performed using Gaussian 09, revision A.02.[53] Graphical outputs of the computational results were generated with the *GaussView* software program (ver. 3.09) developed by Semichem, Inc.[54]

Acknowledgements

This work was supported by grants from the Advanced Low Carbon Technology Research and Development (ALCA) and SENTAN programs from Japan Science Technology Agency (JST) to S. F., the Japan Society for the Promotion of Science (JSPS: Grants 26620154 and 26288037 to K. O., 25288092 and 26105004 to H. Y. and 25-727 to K. M.), and the Green Photonics Project in NAIST sponsored by the MEXT (Japan).

Notes and references

1 (*a*) S. Abrantes, E. Amaral, A. P. Costa, A. A. Shatalov and A. P. Duarte, *Ind. Crops Prod.*, 2007, **25**, 288–293; (*b*) S. H. Zeronian and M. K. Inglesby, *Cellulose*, 1995, **2**, 265–272.

2 L. Li, S. Lee, H. L. Lee and H. J. Youn, *BioResources*, 2011, **6**, 721–736.

3 (*a*) S. Yamazaki, Z. Siroma, H. Senoh, T. Ioroi, N. Fujiwara and K. Yasuda, *J. Power Sources*, 2008, **178**, 20–25; (*b*) R. S. Disselkamp, *Energy Fuels*, 2008, **22**, 2771–2774; (*c*) R. S. Disselkamp, *Int. J. Hydrogen Energy*, 2010, **35**, 1049–1053.

4 S. Fukuzumi, Y. Yamada and K. D. Karlin, *Electrochim. Acta*, 2012, **82**, 493–511.

5 (*a*) Y. Yamada and S. Fukuzumi, *Aust. J. Chem.*, 2014, **67**, 354–364; (*b*) Y. Yamada, M. Yoneda and S. Fukuzumi, *Inorg. Chem.*, 2014, **53**, 1272–1274; (*c*) Y. Yamada, M. Yoneda and S. Fukuzumi, *Chem.–Eur. J.*, 2013, **19**, 11733–11741; (*d*) Y. Yamada, S. Yoshida, T. Honda and S. Fukuzumi, *Energy Environ. Sci.*, 2011, **4**, 2822–2825; (*e*) Y. Yamada, Y. Fukunishi, S. Yamazaki and S. Fukuzumi, *Chem. Commun.*, 2010, **46**, 7334–7336.

6 E. Santacesaria, M. D. Serio, R. Velotti and U. Leone, *Ind. Eng. Chem. Res.*, 1994, **33**, 277–281.

7 M. Fukushima, K. Tatsumi, S. Tanaka and H. Nakamura, *Environ. Sci. Technol.*, 1998, **32**, 3948–3953.

8 S. Liu, K. Mase, C. Bougher, S. D. Hicks, M. M. Abu-Omar and S. Fukuzumi, *Inorg. Chem.*, 2014, **53**, 7780–7788.

9 A. J. Hoffman, E. R. Carraway and M. R. Hoffmann, *Environ. Sci. Technol.*, 1994, **28**, 776–785.

10 (*a*) V. Maurino, C. Minero, G. Mariella and E. Pelizzetti, *Chem. Commun.*, 2005, 2627–2629; (*b*) M. Teranishi, S. Naya and H. Tada, *J. Am. Chem. Soc.*, 2010, **132**, 7850–7851; (*c*) D. Tsukamoto, A. Shiro, Y. Shiraishi, Y. Sugano, S. Ichikawa, S. Tanaka and T. Hirai, *ACS Catal.*, 2012, **2**, 599–603.

11 S. Kato, J. Jung, T. Suenobu and S. Fukuzumi, *Energy Environ. Sci.*, 2013, **6**, 3756–3764.

12 (*a*) Y. Yamada, A. Nomura, K. Ohkubo, T. Suenobu and S. Fukuzumi, *Chem. Commun.*, 2013, **49**, 5132–5134; (*b*) Y. Yamada, A. Nomura, T. Miyahigashi and S. Fukuzumi, *Chem. Commun.*, 2012, **48**, 8329–8331.

13 (*a*) S. Fukuzumi and K. Ohkubo, *Chem. Sci.*, 2013, **4**, 561–574; (*b*) S. Fukuzumi and K. Ohkubo, *Org. Biomol. Chem.*, 2014, **12**, 6059–6071; (*c*) K. Ohkubo and S. Fukuzumi, *Bull. Chem. Soc. Jpn.*, 2009, **82**, 303–315; (*d*) H. Kotani, K. Ohkubo and S. Fukuzumi, *Appl. Catal., B*, 2008, **77**, 317–324; (*e*) K. Ohkubo, R. Iwata, K. Mizushima, K. Souma, Y. Yamamoto, N. Suzuki and S. Fukuzumi, *Chem. Commun.*, 2010, **46**, 601–603.

14 (*a*) K. Mase, K. Ohkubo and S. Fukuzumi, *J. Am. Chem. Soc.*, 2013, **135**, 2800–2808; (*b*) T. Honda, T. Kojima and S. Fukuzumi, *J. Am. Chem. Soc.*, 2012, **134**, 4196–4206; (*c*) S. Fukuzumi, *Chem. Lett.*, 2008, **37**, 808–813; (*d*) S. Fukuzumi, K. Okamoto, C. P. Gros and R. Guilard, *J. Am. Chem. Soc.*, 2004, **126**, 10441–10449; (*e*) S. Fukuzumi, K. Okamoto, Y. Tokuda, C. P. Gros and R. Guilard, *J. Am. Chem. Soc.*, 2004, **126**, 17059–17066.

15 (*a*) S. Fukuzumi, S. Mochizuki and T. Tanaka, *Inorg. Chem.*, 1989, **28**, 2459–2465; (*b*) S. Fukuzumi, S. Mochizuki and T. Tanaka, *Inorg. Chem.*, 1990, **29**, 653–659; (*c*) S. Fukuzumi, S. Mochizuki and T. Tanaka, *J. Chem. Soc., Chem. Commun.*, 1989, 391–392.

16 (*a*) R. McGuire Jr, D. K. Dogutan, T. S. Teets, J. Suntivich, Y. Shao-Horn and D. G. Nocera, *Chem. Sci.*, 2010, **1**, 411–414; (*b*) D. K. Dogutan, S. A. Stoian, R. McGuire Jr, M. Schwalbe, T. S. Teets and D. G. Nocera, *J. Am. Chem. Soc.*, 2011, **133**, 131–140; (*c*) T. S. Teets, T. R. Cook, B. D. McCarthy and D. G. Nocera, *J. Am. Chem. Soc.*, 2011, **133**, 8114–8117.

17 (*a*) F. C. Anson, C. Shi and B. Steiger, *Acc. Chem. Res.*, 1997, **30**, 437–449; (*b*) C. Shi, B. Steiger, M. Yuasa and F. C. Anson, *Inorg. Chem.*, 1997, **36**, 4294–4295; (*c*) C. Shi and F. C. Anson, *Inorg. Chem.*, 1998, **37**, 1037–1043; (*d*) Z. Liu and F. C. Anson, *Inorg. Chem.*, 2000, **39**, 274.

18 (*a*) A. Schechter, M. Stanevsky, A. Mahammed and Z. Gross, *Inorg. Chem.*, 2012, **51**, 22–24; (*b*) J. Masa, K. Ozoemena, W. Schuhmann and J. H. Zagal, *J. Porphyrins Phthalocyanines*, 2012, **16**, 761–784.

19 (*a*) A. J. Olaya, D. Schaming, P.-F. Brevet, H. Nagatani, T. Zimmermann, J. Vanicek, H.-J. Xu, C. P. Gros, J.-M. Barbe and H. H. Girault, *J. Am. Chem. Soc.*, 2012, **134**, 498–506; (*b*) P. Peljo, L. Murtomäki, T. Kallio, H.-J. Xu, M. Meyer, C. P. Gros, J.-M. Barbe, H. H. Girault, K. Laasonen and K. Kontturi, *J. Am. Chem. Soc.*, 2012, **134**, 5974–5984; (*c*) B. Su, I. Hatay, A. Trojánek, Z. Samec, T. Khoury, C. P. Gros, J.-M. Barbe, A. Daina, P.-A. Carrupt and H. H. Girault, *J. Am. Chem. Soc.*, 2010, **132**, 2655–2662.

20 (*a*) S. Fukuzumi, S. Mandal, K. Mase, K. Ohkubo, H. Park, J. Benet-Buchholz, W. Nam and A. Llobet, *J. Am. Chem. Soc.*, 2012, **134**, 9906–9909; (*b*) T. Wada, H. Maki, T. Imamoto, H. Yuki and Y. Miyazato, *Chem. Commun.*, 2013, **49**, 4394–4396.

21 (*a*) K. M. Kadish, L. Fremond, J. Shen, P. Chen, K. Ohkubo, S. Fukuzumi, M. El Ojaimi, C. P. Gros, J.-M. Barbe and R. Guilard, *Inorg. Chem.*, 2009, **48**, 2571–2582; (*b*) P. Chen, H. Lau, B. Habermeyer, C. P. Gros, J.-M. Barbe and K. M. Kadish, *J. Porphyrins Phthalocyanines*, 2011, **15**, 467–479; (*c*) K. M. Kadish, L. Fremond, Z. Ou, J. Shao, C. Shi, F. C. Anson, F. Burdet, C. P. Gros, J.-M. Barbe and R. Guilard, *J. Am. Chem. Soc.*, 2005, **127**, 5625–5631.

22 (*a*) C. J. Chang, Y. Deng, D. G. Nocera, C. Shi, F. C. Anson and C. K. Chang, *Chem. Commun.*, 2000, 1355–1356; (*b*) C. J. Chang, Z. H. Loh, C. Shi, F. C. Anson and D. G. Nocera, *J. Am. Chem. Soc.*, 2004, **126**, 10013–10020.

23 (*a*) E. Askarizadeh, S. B. Yaghoob, D. M. Boghaei, A. M. Slawin and J. B. Love, *Chem. Commun.*, 2010, **46**, 710–712; (*b*) M. Volpe, H. Hartnett, J. W. Leeland, K. Wills, M. Ogunshun, B. J. Duncombe, C. Wilson, A. J. Blake, J. McMaster and J. B. Love, *Inorg. Chem.*, 2009, **48**, 5195–5207.

24 (*a*) R. A. Decréau, J. P. Collman and A. Hosseini, *Chem. Soc. Rev.*, 2010, **39**, 1291–1301; (*b*) J. P. Collman, R. Boulatov, C. J. Sunderland and L. Fu, *Chem. Rev.*, 2004, **104**, 561–588.

25 (*a*) J. Rosenthal and D. G. Nocera, *Acc. Chem. Res.*, 2007, **40**, 543–553; (*b*) M. Schwalbe, D. K. Dogutan, S. A. Stoian, T. S. Teets and D. G. Nocera, *Inorg. Chem.*, 2011, **50**, 1368–1377; (*c*) C. J. Chang, L. L. Chng and D. G. Nocera, *J. Am. Chem. Soc.*, 2003, **125**, 1866–1876.

26 (*a*) Z. Halime, H. Kotani, Y. Li, S. Fukuzumi and K. D. Karlin, *Proc. Natl. Acad. Sci. U. S. A.*, 2011, **108**, 13990–13994; (*b*) E. E. Chufan, S. C. Puiu and K. D. Karlin, *Acc. Chem. Res.*, 2007, **40**, 563–572; (*c*) E. Kim, E. E. Chufan, K. Kamaraj and K. D. Karlin, *Chem. Rev.*, 2004, **104**, 1077–1133.

27 (*a*) C. T. Carver, B. D. Matson and J. M. Mayer, *J. Am. Chem. Soc.*, 2012, **134**, 5444–5447; (*b*) B. D. Matson, C. T. Carver, A. von Ruden, J. Y. Yang, S. Raugei and J. M. Mayer, *Chem. Commun.*, 2012, **48**, 11100–11102; (*c*) J. J. Warren, T. A. Tronic and J. M. Mayer, *Chem. Rev.*, 2010, **110**, 6961–7001.

28 (*a*) S. Kakuda, R. L. Peterson, K. Ohkubo, K. D. Karlin and S. Fukuzumi, *J. Am. Chem. Soc.*, 2013, **135**, 6513–6522; (*b*) D. Das, Y.-M. Lee, K. Ohkubo, W. Nam, K. D. Karlin and S. Fukuzumi, *J. Am. Chem. Soc.*, 2013, **135**, 2825–2834; (*c*) D. Das, Y.-M. Lee, K. Ohkubo, W. Nam, K. D. Karlin and S. Fukuzumi, *J. Am. Chem. Soc.*, 2013, **135**, 4018–4026; (*d*) S. Fukuzumi, L. Tahsini, Y.-M. Lee, K. Ohkubo, W. Nam and K. D. Karlin, *J. Am. Chem. Soc.*, 2012, **134**, 7025–7035.

29 (*a*) S. Fukuzumi and K. D. Karlin, *Coord. Chem. Rev.*, 2013, **257**, 187–195; (*b*) L. Tahsini, H. Kotani, Y.-M. Lee, J. Cho, W. Nam, K. D. Karlin and S. Fukuzumi, *Chem.–Eur. J.*, 2012, **18**, 1084–1093; (*c*) S. Fukuzumi, H. Kotani, H. R. Lucas, K. Doi, T. Suenobu, R. L. Peterson and K. D. Karlin, *J. Am. Chem. Soc.*, 2010, **132**, 6874–6875.

30 (*a*) J. Zhang and F. C. Anson, *J. Electroanal. Chem.*, 1993, **348**, 81–97; (*b*) Y. Lei and F. C. Anson, *Inorg. Chem.*, 1994, **33**, 5003–5009; (*c*) Y. C. Weng, F.-R. F. Fan and A. J. Bard, *J. Am. Chem. Soc.*, 2005, **127**, 17576–17577.

31 (*a*) M. S. Thorum, J. Yadav and A. A. Gewirth, *Angew. Chem., Int. Ed.*, 2009, **48**, 165–167; (*b*) C. C. L. McCrory, A. Devadoss, X. Ottenwaelder, R. D. Lowe, T. D. P. Stack and C. E. D. Chidsey, *J. Am. Chem. Soc.*, 2011, **133**, 3696–3699; (*c*) M. A. Thorseth, C. E. Tornow, E. C. M. Tse and A. A. Gewirth, *Coord. Chem. Rev.*, 2013, **257**, 130–139; (*d*) M. A. Thorseth, C. S. Letko, T. B. Rauchfuss and A. A. Gewirth, *Inorg. Chem.*, 2011, **50**, 6158–6161.

32 C. Kemal, T. W. Chan and T. C. Bruice, *J. Am. Chem. Soc.*, 1977, **99**, 7272–7286.

33 (*a*) K. Gong, F. Du, Z. Xia, M. Durstock and L. Dai, *Science*, 2009, **323**, 760–764; (*b*) S. Wang, D. Yu and L. Dai, *J. Am. Chem. Soc.*, 2011, **133**, 5182–5185.

34 (*a*) Q. Li, B. W. Noffke, Y. Wang, B. Menezes, D. G. Peters, K. Raghavachari and L.-S. Li, *J. Am. Chem. Soc.*, 2014, **136**,

3358–3361; (*b*) Y. Jiao, Y. Zheng, M. Jaroniec and S. Z. Qiao, *J. Am. Chem. Soc.*, 2014, **136**, 4394–4403.

35 L. Wang, A. Ambrosi and M. Pumera, *Angew. Chem., Int. Ed.*, 2013, **52**, 13818–13821.

36 (*a*) S. Shibata, T. Suenobu and S. Fukuzumi, *Angew. Chem., Int. Ed.*, 2013, **52**, 12327–12331; (*b*) S. Fukuzumi, K. Yasui, T. Suenobu, K. Ohkubo, M. Fujitsuka and O. Ito, *J. Phys. Chem. A*, 2001, **105**, 10501–10510; (*c*) S. Fukuzumi, S. Kuroda, T. Goto, K. Ishikawa and T. Tanaka, *J. Chem. Soc., Perkin Trans. 2*, 1989, 1047–1053.

37 (*a*) S. Ghisla and V. Massey, *Eur. J. Biochem.*, 1989, **181**, 1–17; (*b*) T. C. Bruice, *Acc. Chem. Res.*, 1980, **13**, 256–262; (*c*) V. Massey, *J. Biol. Chem.*, 1994, **269**, 22459–22462.

38 S. Fukuzumi and T. Okamoto, *J. Chem. Soc., Chem. Commun.*, 1994, 521–522.

39 (*a*) I. Hatay, B. Su, M. A. Méndez, C. Corminboeuf, T. Khoury, C. P. Gros, M. Bourdillon, M. Meyer, J.-M. Barbe, M. Ersoz, S. Záliš, Z. Samec and H. H. Girault, *J. Am. Chem. Soc.*, 2010, **132**, 13733–13741; (*b*) A. Trojánek, J. Langmaier and Z. Samec, *Electrochim. Acta*, 2012, **82**, 457–462; (*c*) A. Trojánek, J. Langmaier, B. Su, H. H. Girault and Z. Samec, *Electrochem. Commun.*, 2009, **11**, 1940–1943; (*d*) S. Wu and B. Su, *Chem.–Eur. J.*, 2012, **18**, 3169–3173; (*e*) X. Liu, S. Wu and B. Su, *J. Electroanal. Chem.*, 2013, **709**, 26.

40 N. Lopez, D. J. Graham, R. McGuire Jr, G. E. Alliger, Y. Shao-Horn, C. C. Cummins and D. G. Nocera, *Science*, 2012, **335**, 450–453.

41 (*a*) Z.-L. Xue, J. Mack, H. Lu, L. Zhang, X.-Z. You, D. Kuzuhara, M. Stillman, H. Yamada, S. Yamauchi, N. Kobayashi and Z. Shen, *Chem.–Eur. J.*, 2011, **17**, 4396–4407; (*b*) Z.-L. Xue, Z. Shen, J. Mack, D. Kuzuhara, H. Yamada, T. Okujima, N. Ono, X.-Z. You and N. Kobayashi, *J. Am. Chem. Soc.*, 2008, **130**, 16478–16479; (*c*) Z.-L. Xue, D. Kuzuhara, S. Ikeda, Y. Sakakibara, K. Ohkubo, N. Aratani, T. Okujima, H. Uno, S. Fukuzumi and H. Yamada, *Angew. Chem., Int. Ed.*, 2013, **52**, 7306–7309.

42 I. Kaljurand, A. Kütt, L. Sooväli, T. Rodima, V. Mäemets, I. Leito and I. A. Koppel, *J. Org. Chem.*, 2005, **70**, 1019–1028.

43 (*a*) J.-U. Rohde, J.-H. In, M. H. Lim, W. W. Brennessel, M. R. Bukowski, A. Stubna, E. Münck, W. Nam and L. Que Jr, *Science*, 2003, **299**, 1037–1039; (*b*) E. S. Yang, M.-S. Chan and A. C. Wahl, *J. Phys. Chem.*, 1975, **79**, 2049–2051.

44 S. Fukuzumi, T. Suenobu, M. Patz, T. Hirasaka, S. Itoh, M. Fujitsuka and O. Ito, *J. Am. Chem. Soc.*, 1998, **120**, 8060–8068.

45 (*a*) K. Suga, K. Ohkubo and S. Fukuzumi, *J. Phys. Chem. A*, 2005, **109**, 10168–10175; (*b*) H. Kotani, K. Ohkubo and S. Fukuzumi, *J. Am. Chem. Soc.*, 2004, **126**, 15999–16006; (*c*) S. Fukuzumi and K. Ohkubo, *Chem.–Eur. J.*, 2000, **6**, 4532–4535.

46 (*a*) R. N. Bagchi, A. M. Bond, F. Scholz and R. Stösser, *J. Am. Chem. Soc.*, 1989, **111**, 8270–8271; (*b*) M. Bersohn and J. R. Thomas, *J. Am. Chem. Soc.*, 1964, **86**, 959–959; (*c*) J. A. Howard, in *Peroxyl radicals*, ed. Z. B. Alfassi, Wiley, Chichester, 1997, p. 283.

47 (*a*) J. S. Park, E. Karnas, K. Ohkubo, P. Chen, K. M. Kadish, S. Fukuzumi, C. W. Bielawski, T. W. Hudnall, V. M. Lynch and J. L. Sessler, *Science*, 2010, **329**, 1324–1326; (*b*) S. Fukuzumi, K. Ohkubo, Y. Kawashima, D. S. Kim, J. S. Park, A. Jana, V. Lynch, D. Kim and J. L. Sessler, *J. Am. Chem. Soc.*, 2011, **133**, 15938–15941.

48 W. L. F. Armarego and C. L. L. Chai, *Purification of Laboratory Chemicals*, Pergamon Press, Oxford, 7th edn, 2013.

49 S. Fukuzumi, S. Kuroda and T. Tanaka, *J. Am. Chem. Soc.*, 1985, **107**, 3020–3027.

50 (*a*) S. Fukuzumi, H. Imahori, H. Yamada, M. E. El-Khouly, M. Fujitsuka, O. Ito and D. M. Guldi, *J. Am. Chem. Soc.*, 2001, **123**, 2571–2575; (*b*) S. Fukuzumi, M. Ishikawa and T. Tanaka, *J. Chem. Soc., Perkin Trans. 2*, 1989, 1037–1045.

51 C. K. Mann and K. K. Barnes, in *Electrochemical Reactions in Non-Aqueous Systems*, Mercel Dekker, New York, 1970.

52 A. D. Becke, *J. Chem. Phys.*, 1993, **98**, 5648–5652.

53 M. J. Frisch, G. W. Trucks, H. B. Schlegel, G. E. Scuseria, M. A. Robb, J. R. Cheeseman, G. Scalmani, V. Barone, B. Mennucci, G. A. Petersson, H. Nakatsuji, M. Caricato, X. Li, H. P. Hratchian, A. F. Izmaylov, J. Bloino, G. Zheng, J. L. Sonnenberg, M. Hada, M. Ehara, K. Toyota, R. Fukuda, J. Hasegawa, M. Ishida, T. Nakajima, Y. Honda, O. Kitao, H. Nakai, T. Vreven, J. A. Montgomery Jr, J. E. Peralta, F. Ogliaro, M. Bearpark, J. J. Heyd, E. Brothers, K. N. Kudin, V. N. Staroverov, R. Kobayashi, J. Normand, K. Raghavachari, A. Rendell, J. C. Burant, S. S. Iyengar, J. Tomasi, M. Cossi, N. Rega, J. M. Millam, M. Klene, J. E. Knox, J. B. Cross, V. Bakken, C. Adamo, J. Jaramillo, R. Gomperts, R. E. Stratmann, O. Yazyev, A. J. Austin, R. Cammi, C. Pomelli, J. W. Ochterski, R. L. Martin, K. Morokuma, V. G. Zakrzewski, G. A. Voth, P. Salvador, J. J. Dannenberg, S. Dapprich, A. D. Daniels, O. Farkas, J. B. Foresman, J. V. Ortiz, J. Cioslowski and D. J. Fox, *Gaussian 09, revision A.02*, Gaussian, Inc., Wallingford, CT, 2009.

54 R. Dennington II, T. Keith, J. Millam, K. Eppinnett, W. L. Hovell and R. Gilliland, *Gaussview*, Semichem, Inc., Shawnee Mission, KS, 2003.

